Eur. Phys. J. D (2020) 74: 88
https://doi.org/10.1140/epjd/e2020-100481-9

THE EUROPEAN PHYSICAL JOURNAL D

Topical Review

Electron impact ionization and fragmentation of biofuels*

M. Cristina A. Lopes[1,a], Wesley A. D. Pires[1], Kate L. Nixon[2], Raony A. A. Amorim[1], Daniel G. M. da Silva[1], Anne C. P. Fernandes[1], Santunu Ghosh[1], Darryl B. Jones[3], Laurence Campbell[3], Rafael F. C. Neves[1,4], Humberto V. Duque[1,4], Gustavo García[5], Francisco Blanco[6], and Michael J. Brunger[3,7]

[1] Departamento de Física, Universidade Federal de Juiz de Fora, Juiz de Fora, MG 36036-900, Brazil
[2] Wolverhampton School of Sciences, University of Wolverhampton, Wolverhampton WV1 1LY, UK
[3] College of Science and Engineering, Flinders University, GPO Box 2100, Adelaide, SA 5001, Australia
[4] Instituto Federal do Sul de Minas Gerais, Campus Poços de Caldas, Poços de Caldas, MG 37713-100, Brazil
[5] Instituto de Física Fundamental, Consejo Superior de Investigaciones Científicas (CSIC), Serrano 113-bis, 28006 Madrid, Spain
[6] Departamento de Estructura de la Materia, Física Térmica y Electrónica, Universidad Complutense de Madrid, 28040 Madrid, Spain
[7] Dept of Actuarial Science and Applied Statistics, Faculty of Business and Information Science, UCSI University, Kuala Lumpur 56000, Malaysia

Received 30 September 2019 / Received in final form 19 March 2020
Published online 5 May 2020

Abstract. We present in this article, a review of our recent experimental and theoretical studies published in the literature on electron impact ionization and fragmentation of the primary alcohols methanol, ethanol, 1-propanol and 1-butanol (C_1–C_4). We discuss the mass spectra (MS) of these alcohols, measured for the electron impact energy of 70 eV and also, total (TICS) and partial (PICS) ionization cross sections in the energy range from 10 to 100 eV, which revealed the probability of forming different cations, by either direct or dissociative ionization. These experimental TICS are summarized together with theoretical values, calculated using the Binary-encounter Bethe (BEB) and the independent atom model with the screening corrected additivity rule (IAM-SCAR) methods. Additionally, we compared data of appearance energies – AE and discussed the application of the extended Wannier theory to PICS in order to produce the ionization and ionic fragmentation thresholds for the electron impact of these alcohols.

1 Introduction

We have developed over the last five years a research program aimed at the study of electron collisions with biofuels, using the mass spectrometry technique [1–4]. This work is part of a broader analysis of the ionization and ionic fragmentation of these fuels using electron impact in the energy range from 10 to 100 eV, where we review previously published data in the literature. The reason behind the renewed interest of the academic community in investigating these alcohols is the well-known fact that the demand for fuels is growing worldwide, as we apply them in different technologies for our comfort and well-being. However, it is also an unquestionable fact that this use of fossil fuel in motor vehicles factories, power generators, etc., has had quite serious consequences for the environment and consequently, for our health and quality of life, especially in large cities [5,6]. To qualify and quantify this problem, it is only necessary to mention that nowadays more than 4 million people die every year worldwide as a direct or indirect consequence of air pollution [7]. Therefore our modern lifestyle, requiring large amounts of fuel must be questioned and rethought, not only from a personal point of view, but mainly through new government policies, to replace fossil fuels with less aggressive alternatives for human beings and the environment as a whole. In this sense, it is crucial to develop several technological fronts to replace petroleum-based fuels, such as Fuel Cell Electric Vehicles (FCEVs), Electric Vehicles (EVs), and Biofuel vehicles [8]. A biofuel is a good alternative [9,10] as its use is a carbon neutral process [9], which means that the amount of carbon dioxide released into the atmosphere in its burning is reabsorbed in the photosynthesis process, carried out by the plants which will be used as raw material in biofuel production, which does not occur with fossil fuels. Using petroleum fuels that have been sequestered for millions of years in the earth pollutants

* Contribution to the Topical Issue "Low-Energy Positron and Positronium Physics and Electron-Molecule Collisions and Swarms (POSMOL 2019)", edited by Michael Brunger, David Cassidy, Saša Dujko, Dragana Marić, Joan Marler, James Sullivan, Juraj Fedor.

[a] e-mail: cristina.lopes@ufjf.edu.br

such as CO_2 and CO are emitted into the atmosphere, thus seriously contributing to the greenhouse effect, acid rain and other environmental problems [8,11]. For example, due to the incomplete burning of these fossil fuels in the combustion process, carcinogenic compounds, such as benzene, are also released into the atmosphere [12].

Although ethanol is the most widely used and currently known biofuel, 1-butanol has numerous advantages over it (and methanol and 1-propanol), namely:

(i) due to its lower oxygen content (22%), its burning is cleaner;
(ii) having a longer carbon chain gives it a higher energy density and makes it less volatile than ethanol [12,13];
(iii) its lower energy density than gasoline, shown in Table 1, and its non-hygroscopic and non-corrosive nature (in contrast to gasoline and ethanol) minimize the problem of its storage and distribution;
(iv) its energy density is 27 MJ/L while that of ethanol is 20 MJ/L, which means that 1-butanol releases more energy during the internal combustion process, i.e. with the same amount of fuel a vehicle travels further [12];
(v) 1-Butanol has a higher octane rating (87–104 AKI – ADI, depending on the isomer) [13,14] compared to ethanol (99.5 AKI) and is close to gasoline (85–96 AKI) (Tab. 1). The higher the octane rating, the greater the fuel's ability to withstand high pressure and temperature conditions without spontaneous explosion. This fact is quite important in engines running on internal combustion as an explosion at a stage prior to spark emission from the spark plug, causes the engine to lose its efficiency. Consequently, the use of 1-butanol, in principle, means that there is no loss of mechanical efficiency [11,12,15];
(vi) its auto-ignition temperature 343 °C, lower than ethanol (434 °C) as shown in Table 1, facilitates ignition in low temperature regions [16];
(vii) the low vapour pressure of butanol makes it a low flammability fuel. This makes butanol a potentially safer fuel compared to methanol, ethanol and gasoline, which are all flammable and potentially explosive;
(viii) butanol has handling characteristics similar to gasoline and ethanol and therefore the same consolidated production, transportation and marketing infrastructure can be used and does not demand large new retooling investments.

The main problem found regarding the intensive use of 1-butanol as an alternative vehicle fuel so far, is that it can only be produced from genetically engineered algae and the fermentation of renewable biomass [11,12,15,17]. Hence, it is not yet produced on an industrial scale. Thus, knowing in detail its characteristics and potential compared to other fuels, has made clear the need for further research to enable the development of new technologies for its large scale production and application.

In order to use biofuels, such as the C_1–C_4 alcohols, it is necessary to understand, compare and optimize the process in internal combustion engines. Their spark-ignition properties should be investigated and modelled to determine the parameters to be applied in the development of new technologies. These modelling studies may provide the optimum parameters to be used for more economical engines, which will use the poorest fuel-air mixtures, where a complete burning of fuel would release smaller compounds into the atmosphere, resulting in less polluting vehicles. To perform this modelling, it is necessary to know all the species present and created in the spark-ignition process [18], involving positive and negative ions, radicals and neutral fragments and the rate of contribution or production of each species, which in turn, are related to their cross sections (CSs), of which the PICS and TICS are the subject of this review.

The first recorded study of electron collisions with primary alcohols was published by Schmieder [19] in 1930, reporting TCS measurements for methanol and ethanol in the low energy region. The interest of the scientific community starts to become more extensive only after 2003 [20], most likely due to the technological, environmental and human health appeal for the use of alcohols as biofuels, instead of fossil fuels. These experimental and theoretical investigations include total (TCS) [19,21–29], elastic differential (EDCS), integral (ICS) and momentum transfer cross sections (MTCS) [16,26,30–32], absolute total ionization cross sections (TICS) [1,2,4,16,20,33–40], partial ionization cross sections (PICS) [1–3,20,33–38,41,42], appearance energies (AEs) determinations for a selection of the cations generated by electron impact ionization [1,2,4,41,43,44] and also the mass spectra acquisition [1–3,34,41–43,45–47], as are summarized in Table 2. This table reveals that as the alcohol carbon chain increases in length, there is less research done, which is most likely due to the difficulty in carrying out these studies as the molecules become less volatile. In addition, a greater adherence to the inner walls of the measuring apparatus is observed as the size of the alcohol increases, making it difficult to pump out the residual gas, even when baking the vacuum chamber. This also results in a deterioration in the electron optics performance of the apparatus, and also a decrease in the lifetime of the electron source filament and the detector. Theoretically the difficulties appear when the number of degrees of freedom involved in the problem increases. This is directly linked to the size of the molecule, where the opening of many reaction channels, due to the electron-molecule collisions, increases the time required to perform the calculations.

We presented here a review of experimental and theoretical studies on electron impact ionization and fragmentation of the biofuels methanol, ethanol, 1-propanol and 1-butanol, which reveals a series of trends as the size and complexity of molecules increases. The mass spectra (MS) for these primary alcohols (C_1–C_4), recorded at 70 eV electron impact energy, are discussed together with the PICS, from which the TICS were derived. We also examine theoretical Binary-encounter Bethe (BEB) and independent atom model with the screening corrected additivity rule (IAM-SCAR) TICS results, as calculated

Table 1. Comparison of the octane rating, energy density and auto-ignition temperature of the primary alcohols with gasoline.

	Gasoline	Methanol	Ethanol	1-Propanol	1-Butanol
Octane rating	85–96 AKI	106 AKI	99,5 AKI	108 AKI	87–104 AKI
Energy density	33 MJ/L[12]	18 MJ/L	20 MJ/L	24 MJ/L	27 MJ/L[12]
Auto-ignition temperature	246 °C	370 °C	434 °C	405 °C	343 °C

Table 2. Studies performed up to now for electron collisions with the primary alcohols methanol, ethanol, 1-propanol and 1-butanol, reporting data of TCS, EDCS, ICS, MTCS, PICS, TICS, AEs and MS. The experimental studies are marked with the upper index (e), while the theoretical ones are denoted by the index (t). The studies performed by our research group are shown in bold in this table, highlighting our contribution to the investigation of primary alcohols.

	Methanol	Ethanol	1-Propanol	1-Butanol
TCS	Schmieder-1930^{e}[19] Sueoka-1985^{e} [21] Szmytkowski-1995^{e}[22] Vinodkumar-2008^{t} [23] **Silva-2010**^{e} [24] Tan-2011^{t}[25] Lee-2012^{t}[26] Vinodkumar-2013^{t}[27]	Schmieder-1930^{e} [19] **Silva-2010**^{e} [24] Tan-2011^{t} [25] Lee-2012^{t} [26]	**Silva-2018**^{e,t} [28]	**Gomes-2019**^{e,t} [29]
EDCS, ICS, MTCS	Bouchiha-2007^{e,t} [30] Khakoo-2008^{e,t} [31] Sugohara-2011^{e,t} [32] Lee-2013^{t} [26]	Khakoo-2008^{e,t} [31] Lee-2013^{e,t} [26]	Khakoo-2008^{e,t} [16]	Khakoo-2008^{e,t} [16]
TICS	Srivastava-1996^{e} [34] Duric-1998^{e} [33] Deutsch-1998^{t} [35] Rejoub-2003^{e} [20] Hudson-2003^{e} [36] Pal -2004^{t} [37] Vinodkumar-2011^{t} [38] **Nixon-2016**^{e} [1]	Duric -1998^{e} [33] Deutsch-1998^{t} [35] Rejoub-2003^{e} [20] Hudson-2003^{e,t} [36] Vinodkumar-2011^{t} [38] **Nixon-2016**^{e} [1]	Duric -1998^{e} [33] Hudson-2003^{e,t} [36] Rejoub-2003^{e} [20] Khakoo-2008^{e,t} [16] Vinodkumar-2011^{t} [38] Bull-2012^{t} [39] **Pires-2018**^{e,t} [2]	Hudson-2003^{e,t} [36] Uddin-2018^{t} [40] **Ghosh-2018**^{e,t} [4]
PICS	Duric-1989^{e} [33] Srivastava-1996^{e} [34] Deutsch-1998^{t} [35] Hudson-2003^{e} [36] Rejoub-2003^{e} [20] Pal-2004^{t} [37] Zavilopulo-2005^{e} [41] Douglas-2009^{e} [42] Vinodkumar-2011^{t} [38] **Nixon-2016**^{e} [1]	Rejoub-2003^{e} [20] **Nixon-2016**^{e} [1]	Rejoub-2003^{e} [20] **Pires-2018**^{e} [2]	Rejoub-2003^{e}[20] **Pires-2018**^{e,t} [3]
AEs	Cummings-1940^{e} [43] Zavilopulo-2005^{e} [41] **Nixon-2016**^{e} [1]	Cummings-1940^{e} [43] **Nixon-2016**^{e} [1]	Williams-1968 [44] **Pires-2018**^{e,t} [2]	**Ghosh-2018**^{e,t} [4]
MS	**Nixon-2016**^{e} [1] Cummings-1940^{e} [43] Srivastava-1996^{e} [34] Rejoub-2003^{e} [20] Douglas-2009^{e} [42] Szot -2013^{e} [45]	Rejoub-2003^{e} [20] Szot -2013^{e} [46] **Nixon-2016**^{e} [1]	Rejoub-2003^{e} [20] Maccoll-2017^{e,t} [47] **Pires-2017**^{e,t} [2]	Friedel-1956^{e} [47] Zavilopulo-2005^{e}[41] **Pires-2018**^{e,t} [3]

in references [2,4]. Appearance energies (AEs) for the most intense cations formed in electron collisions with the studied alcohols were also compared and discussed.

The structure of the remainder of this paper is as follows. In Section 2 we describe the relevant experimental and theoretical methods used in the mass spectra acquisition, PICS and TICS investigations, while in Section 3 the mass spectra, PICS and TICS, as well as the AEs, are presented and discussed. Finally, some conclusions from this review are summarised in Section 4.

2 Experimental and theoretical methods

Mass spectrometry is an outstanding analytical method applied to investigate the electron impact ionic fragmentation of molecules, which has progressed extremely rapidly during the last few decades, leading to the improvements in its resolution, sensitivity, mass range and accuracy of produced data. These mass spectrometers essentially include an ionization source, an analyser applied for the separation of ions according to their mass-to-charge ratio, which may be based on different principles, i.e. electric or magnetic sectors, quadrupoles, ion-traps, time-of-flight (TOF) or even hybrid instruments such as the quadrupole TOF instrument [49], and the detector. In our studies for the C_1–C_4 alcohols, reported by [1–4], a Hiden Analytical quadrupole mass spectrometer (QMS) [50], which is capable of measuring masses up to 300 amu and with 1 amu resolution, was used. In these experiments the residual gas analysing (RGA) mode of this spectrometer, which applies its internal ionization source to create ions by electron impact from the target was used. The performance of the apparatus was carefully checked considering the mass dependence over the mass range studied, i.e. the mass dependent transmission of the QMS, the uniform extraction to the mass filter for all cations, the operating pressure stability, the incident electron current stability and the detected ion signal, producing very reliable data, as we reported in [1–4]. These data were compared with experimental results reported in the literature, obtained by the application of different techniques, i.e. Srivastava et al. [34] whose apparatus employed a QMS a mass filter, Rejoub et al. [20] and Douglas et al. [42] who used different versions of TOF mass filters, Hudson et al. [36] who used a total ionization cell to measure the absolute TICS with no mass selectivity, Zavilopulo et al. [41] whose apparatus employed a monopole mass selector, Cummings and Bleakney [43] who used a 180° mass selector and Szot et al. [45] who used a magnetic sector field followed by the electric sector field analyzer.

Theoretical calculations for the total ionization cross sections for 1-propanol and 1-butanol were also performed [2,4], within the BEB [18] and IAM-SCAR frameworks [51,52]. These two methods have been described in some detail in ours previous articles [2,4], so that only a brief description need be given here for completeness. The total ionization cross sections at the BEB level of approximation [18] were obtained by summing up the partial ionization cross sections, Q_i, over the N-occupied orbitals, given by:

$$Q_i(t_i) = \frac{4\pi a_o^2 N_i}{t_i + u_i + 1}\left(\frac{R}{B_i}\right)^2\left[\frac{\ln t_i}{2}\left(1 - \frac{1}{t_i^2}\right) + 1 - \frac{1}{t_i} - \frac{\ln t_i}{t_i + 1}\right], \quad (1)$$

where N_i, R and a_o are respectively, the orbital occupation number, the Rydberg constant and the Bohr radius. In this equation, the binding energy of the ionized orbital B_i, is used to scale the electron impact energy (E_o) and orbital kinetic energy (U_i), $t_i = \frac{E_o}{B_i}$ and $u_i = \frac{U_i}{B_i}$, respectively. In this approximation, the geometry of 1-propanol and 1-butanol were optimized at the B3LYP/aug-cc-pVDZ level for the most abundant trans-trans, gauche-trans and trans-gauche conformers [53] using Gaussian 09 [54]. Single Point calculations were then performed using the Outer Valence Greens' function method and B3LYP levels, again with the aug-cc – pVDZ basis.

The cross sections obtained using the IAM-SCAR framework [51,52] are derived by considering the sum of individual electron scattering processes from each individual atom present within the target molecule, with a screening correction derived from the target molecule's geometry implemented to describe the interactions between individual atoms within the molecule. The electron scattering cross sections for a particular atom are obtained using an optical model based on a potential scattering approach, where the local complex potential is given by:

$$V(r) = V_s(r) + V_{\rm ex}(r) + V_p(r) + iV_a(r). \quad (2)$$

In this equation $V_s(r)$ is the Hartree-Fock potential of the target [55], $V_{\rm ex}(r)$ is the electron exchange interaction [56], $V_p(r)$ is the dipole polarization [57] and $iV_a(r)$ is the complex absorption potential [58].

3 Results and discussion

The mass spectra reported by our research group [1–3] compared to data reported in the literature for C_1–C_4 alcohols, measured at 70 eV electron impact energy, are shown in Figure 1, and assignments for the fragments formed are listed in Table 3, along with their relative abundances with respect to the base peak at m = 31 amu and their standard deviations. The assignments of the formed cations were carried out assuming that all of the ions in the mass spectrum were singly ionized [1–3]. The corresponding abundances and related errors of [1–3], were obtained after the background signal subtraction, with the average spectrum being normalised to the base peak corresponding to oxonium, CH_2OH^+, observed at m/z = 31. This ion, which constitutes a signature of the primary alcohols, has a resonance stabilized structure, which contributes to its relatively high intensity [59,60]. All the C_1–C_4 spectra [1–3] compare quite well with the relative ratios from NIST [61]. Our methanol spectrum also compares quite well with data from Srivastava et al. [34], Douglas and Price [42] and Cummings and Bleakney [43], although there are some differences noted for data at masses 1 amu, 15 amu, 29 amu and 32 amu reported by [42] and for masses 15 amu, 28 amu, 29 amu, 32 amu reported by [43]. The data obtained by Szot et al. [45] compare well to our data in the mass region above 28 amu for methanol, while

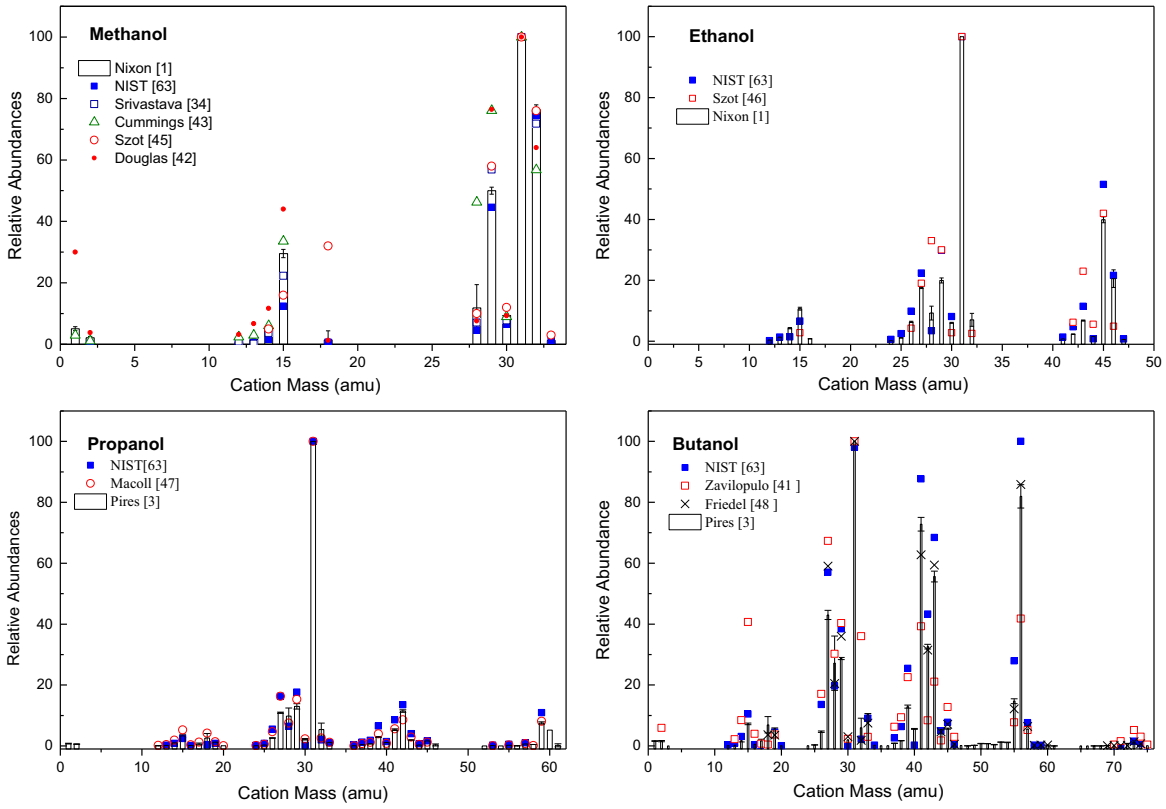

Fig. 1. Mass spectra of methanol, ethanol, 1-propanol and 1-butanol, obtained at 70 eV electron impact energy, measured with a Hiden quadrupole mass spectrometer [1–4], compared with the literature. The parent ion for methanol (CH_4O^+) is observed at 32 amu, while for ethanol ($C_2H_6O^+$) at 46 amu, for 1-propanol ($C_3H_8O^+$) at 60 amu and for 1-butanol ($C_4H_{10}O^+$) at 74 amu. The value of the ratio m/z in these spectra is equal to the value of the mass, given that all the cations detected here are singly ionized [1–4]. The spectra for methanol, ethanol and 1-propanol, reported by [1–3], are placed on an absolute scale through normalisation to the absolute measurement of Rejoub et al. [20], and for 1-butanol to the absolute data of Hudson et al. [36].

for ethanol better agreement was found for masses 15 amu, 26 amu, 27 amu, 30 amu, 32 amu, 42 amu and 45 amu. We found good agreement between our 1-propanol spectrum [3] and the relative ratio intensities from Maccoll [47], as can be seen in Figure 1. The butanol spectrum is mainly characterized by the dispersion of data recorded by all authors, with just few agreements. In our spectrum of 1-butanol [3] a large number of low intensity cations peaks were registered, which were not previously observed by Zavilopulo et al. [41] and Friedel et al. [48], very likely due the higher sensitivity of our apparatus.

The absolute partial ionization cross sections (PICS) were measured for 9 cation masses of methanol [1], constituting 96% of the total ion contributions to its mass spectrum generated by electrons with impact energy 70 eV. We also measured the PICS for 19 cation masses of ethanol [1], which account for 90% of the cations produced, for 32 cations of 1-propanol [2], constituting 96.6% of the cations produced, and for 38 cations of 1-butanol [3], which account for 96.6% of the total ion contributions observed in its spectrum. By summing these PICS for each alcohol, were obtained their total ionization cross sections (TICS) [1–4] in the energy range 10–100 eV, which are shown in Figure 2. The absolute scales of the experimental TICS for methanol, ethanol and 1-propanol have been determined through a single point normalization of our data (at 70 eV) to that of Rejoub et al. [20], while for 1-butanol, normalisation was achieved against the absolute data of Hudson et al. [36].

In addition to the experimental investigations, theoretical TICS were also calculated using the BEB [18] and IAM-SCAR [51,52] methods. Figure 2 shows the comparison of methanol and ethanol TICS experimental data reported by Nixon et al. [1], and theoretical results reported by Hudson et al [36]. This figure also shows the experimental and theoretical TICS for 1-propanol from [2] and for 1-butanol from [4]. The experimental TICS for methanol from [1] are in very good agreement with data from Hudson et al. [36], over all electron impact energies investigated. It is important to note that the observed concordances between the values of the experimental TICS (obtained by adding the PICS) and the theoretical results, confirm the accuracy of the experimental records of the PICS of [1–4]. We can also observe a very good agreement between the ethanol TICS reported by us in [1] and the Hudson et al. data for energies above 55 eV. The 1-propanol TICS experimental data [2] are in quite good agreement with the BEB calculation reported in [2]. However, at energies above 60 eV some discrepancies are observed between the measured and BEB calculated

Table 3. Comparison of the relative abundances of the cations generated by electron impact on methanol [1], ethanol [1], 1-propanol [2] and 1-butanol [3] using an electron energy of 70 eV. The relative abundance is expressed with respect to the base peak observed at 31 amu for all alcohols, and the error is the standard deviation on that average determined after the normalization process. Ab. in the table refers to the abundance of the formed fragment.

Methanol				Ethanol				Propanol				Butanol			
Cation Identity	Mass (amu)	Ab.	Error	Cation Identity	Mass (amu)	Ab.	Error	Cation Identity	Mass (amu)	Ab.	Error	Cation Identity	Mass (amu)	Ab.	Error
H^+	1	5.10	0.65	H^+	1	2.42	0.47	H^+	1	0.77	0.12	H^+	1	1.58	0.12
H_2^+	2	2.14	0.45	H_2^+	2	1.07	0.31	H_2^+	2	0.58	0.07	H_2^+	2	1.56	0.20
												H_3^+	3	0.01	0.00
C^+	12	0.92	0.05	C^+	12	0.43	0.02	C^+	12	0.09	0.02	C^+	12	0.12	0.01
CH^+	13	1.65	0.11	CH^+	13	1.37	0.07	CH^+	13	0.21	0.03	CH^+	13	0.25	0.03
CH_2^+	14	5.36	0.59	CH_2^+	14	4.29	0.21	CH_2^+	14	1.03	0.16	CH_2^+	14	1.70	0.41
CH_3^+	15	29.57	1.35	CH_3^+	15	10.69	0.45	CH_3^+	15	3.30	0.57	CH_3^+	15	7.22	0.26
				O^+ or CH_4^+	16	0.83	0.04	O^+ or CH_4^+	16	0.21	0.06	CH_4^+ or O^+	16	0.52	0.14
				OH^+	17	3.23	0.54	OH^+	17	0.62	0.34	OH^+	17	1.65	0.56
H_2O^+	18	1.48	2.92	H_2O^+	18	13.6	1.18	H_2O^+	18	2.58	1.50	H_2O^+	18	6.93	2.69
				H_3O^+	19	5.89	0.30	H_3O^+	19	1.27	0.06	H_3O^+	19	5.69	0.20
								H_2DO^+	20	0.05	0.00	H_2DO^+	20	0.06	0.02
				C_2^+	24	0.20	0.01	C_2^+	24	0.05	0.00	C_2^+	24	0.05	0.00
				C_2H^+	25	1.13	0.04	C_2H^+	25	0.31	0.02	C_2H^+	25	0.32	0.02
				$C_2H_2^+$	26	6.35	0.19	$C_2H_2^+$	26	2.61	0.07	$C_2H_2^+$	26	4.65	0.23
				$C_2H_3^+$	27	17.71	0.43	$C_2H_3^+$	27	10.91	0.22	$C_2H_3^+$	27	43.00	1.50
CO^+	28	11.86	7.55	CO^+ or $C_2H_4^+$	28	9.25	2.26	CO^+ or $C_2H_4^+$	28	9.79	2.66	CO^+ or $C_2H_4^+$	28	27.17	8.90
COH^+	29	50.0	1.15	COH^+ or $C_2H_5^+$	29	19.98	0.82	COH^+ or $C_2H_5^+$	29	13.00	0.88	COH^+ or $C_2H_5^+$	29	28.68	0.36
CH_2O^+	30	9.44	0.43	CH_2O^+ or $C_2H_6^+$	30	6.05	0.15	CH_2O^+ or $C_2H_6^+$	30	2.19	0.23	CH_2O^+ or $C_2H_6^+$	30	2.03	0.08
CH_3O^+	31	100.0	0.001	CH_3O^+	31	100	0.00	CH_3O^+	31	100	0.00	CH_3O^+	31	100	0.00
CH_4O^+	32	76.35	1.56	CH_4O^+	32	7.02	2.14	CH_4O^+	32	5.38	2.11	CH_4O^+	32	5.94	3.16
$^{13}CH_3OH^+$	33	1.30	0.10	CH_5O^+	33	0.18	0.01	CH_5O^+	33	1.17	0.03	CH_5O^+	33	10.28	0.35
												CH_6O^+	34	0.23	0.01
												CH_7O^+	35	0.06	0.00
								C_3^+	36	0.07	0.00	C_3^+	36	0.07	0.00
								C_3H^+	37	0.44	0.02	C_3H^+	37	0.85	0.03
								$C_3H_2^+$	38	0.73	0.05	$C_3H_2^+$	38	1.71	0.06
								$C_3H_3^+$	39	2.92	0.13	$C_3H_3^+$	39	12.90	0.49
								C_2O^+ or $C_3H_4^+$	40	1.11	0.10	C_2O^+ or $C_3H_4^+$	40	5.59	0.15
				C_2HO^+	41	0.78	0.10	C_2HO^+ or $C_3H_5^+$	41	5.33	0.27	C_2HO^+ or $C_3H_5^+$	41	72.78	2.24
				$C_2H_2O^+$	42	2.32	0.07	$C_2H_2O^+$ or $C_3H_6^+$	42	11.45	0.4	$C_2H_2O^+$ or $C_3H_6^+$	42	32.60	0.78
				$C_2H_3O^+$	43	6.79	0.18	$C_2H_3O^+$ or $C_3H_7^+$	43	1.95	0.09	$C_2H_3O^+$ or $C_3H_7^+$	43	55.62	1.77
				$C_2H_4O^+$	44	1.51	0.05	$C_2H_4O^+$ or $C_3H_8^+$	44	0.31	0.12	$C_2H_4O^+$ or $C_3H_8^+$	44	5.44	0.11
				$C_2H_5O^+$	45	39.89	0.99	$C_2H_5O^+$	45	1.63	0.69	$C_2H_5O^+$	45	5.68	0.19
				$C_2H_6O^+$	46	20.56	2.89	$C_2H_6O^+$	46	0.33	0.35	$C_2H_6O^+$	46	0.64	0.04
				$^{12}C^{13}CH_6O^+$	47	0.60	0.08					$C_2H_7O^+$	47	0.11	0.00
												C_4^+	48	0.03	0.01
												C_4H^+	49	0.20	0.01
												$C_4H_2^+$	50	0.79	0.05
												$C_4H_3^+$	51	0.75	0.05
								C_3O^+	52	0.02	0.00	$C_4H_4^+$ or C_3O^+	52	0.42	0.04
								C_3HO^+	53	0.11	0.00	$C_4H_5^+$ or C_3HO^+	53	1.24	0.07
								$C_3H_2O^+$	54	0.02	0.00	$C_4H_6^+$ or $C_3H_2O^+$	54	1.15	0.09
								$C_3H_3O^+$	55	0.23	0.01	$C_4H_7^+$ or $C_3H_3O^+$	55	14.68	0.82
								$C_3H_4O^+$	56	0.08	0.01	$C_4H_8^+$ or $C_3H_4O^+$	56	81.93	3.84
								$C_3H_5O^+$	57	0.68	0.06	$C_4H_9^+$ or $C_3H_5O^+$	57	5.55	0.27
								$C_3H_6O^+$	58	0.48	0.02	$C_3H_6O^+$	58	0.17	0.02
								$C_3H_7O^+$	59	7.51	0.39	$C_3H_7O^+$	59	0.33	0.16
								$C_3H_8O^+$	60	5.20	0.50	$C_3H_8O^+$	60	0.16	0.14
								$^{12}C_2^{13}CH_8O^+$	61	0.20	0.02	$C_3H_9O^+$	61	0.01	0.01
												C_4HO^+	65	0.01	0.00
												$C_4H_2O^+$	66	0.02	0.00
												$C_4H_3O^+$	67	0.01	0.01
												$C_4H_4O^+$	68	0.01	0.01
												$C_4H_5O^+$	69	0.09	0.02
												$C_4H_6O^+$	70	0.12	0.03
												$C_4H_7O^+$	71	0.13	0.03
												$C_4H_8O^+$	72	0.78	0.06
												$C_4H_9O^+$	73	1.39	0.11
												$C_4H_{10}O^+$	74	0.73	0.08
												$^{12}C_3^{13}CH_{10}O^+$	75	0.04	0.01

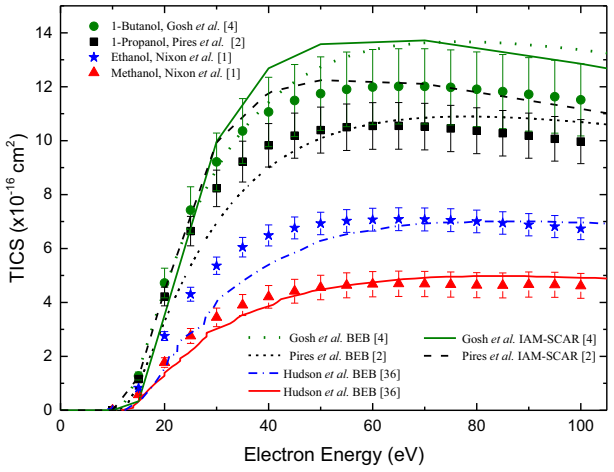

Fig. 2. Comparison of the absolute total ionization cross sections (TICS) of methanol [1,36], ethanol [1,36], 1-propanol [2], 1-butanol [4] in the 10–100 eV impact electron energy range. The TICS, obtained by the sum of the absolute PICS for all the cations observed in the electron collisions, are shown with their errors being the mean square root of the sum of squares of statistical errors as well as inheriting the uncertainty in the absolute data used in the normalization. See also legend in figure.

TICS in [2], given that the experimental results somewhat underestimate the true TICS due to the omission of the contribution from the lighter cations in [2]. The IAM-SCAR calculation for 1-propanol presents better qualitative agreement, although it still overestimates the TICS for energies above 30 eV. The BEB TICS for 1-butanol, reported in [3], give good agreement with the experimental results up to energies of 50 eV, to within experimental uncertainty. At higher energies, the BEB calculation is somewhat larger in magnitude than the experimental data [3], which may again reflect that some of the PICSs are not included in obtaining the experimental TICS. The measured 1-butanol TICS is also in reasonable agreement with the IAM-SCAR calculation, both reported in [3].

The IAM-SCAR calculation gives a somewhat larger cross section than that obtained within the BEB formalism at energies between 30 and 60 eV, but gives smaller values than the BEB as the incident electron energy increases toward 100 eV. Within the IAM-SCAR formalism, the calculation includes contributions from other absorption channels, such as discrete electronic-state excitation and neutral dissociation, which may lead to a higher cross section than that seen at the BEB level. At larger impact energies, above 80 eV, the IAM-SCAR TICS is in good agreement with the two sets of experimental values, reflecting the fact that the approximations employed within the IAM-SCAR formalism become more realistic with increasing incident electron energy.

It is apparent from Figure 2 that the TICS for the primary alcohols increase with the size of the molecule, with 1-butanol having a larger value than the other three alcohols. The observed shapes of the TICS for the C_1–C_4 alcohols are also quite consistent for each molecule, over the threshold to 100 eV energy range. As Hudson et al. [36] have previously shown that the maximum intensity of the TICS can be described through a relationship between the molecular dipole-polarizability and the ionization threshold, the similar shape observed for the present C_1–C_4 alcohols suggests that the characteristic primary alcohol TICS shape might be rescaled, based on the empirical TICS maximum determined from a relevant dipole polarizability and ionization threshold, to approximate the TICS for the larger primary alcohols whose cross sections are currently unknown.

In the left pane of Figure 3, a comparison is shown of the absolute partial ionization cross sections (PICS) of the parent ions of methanol (CH_4O^+), ethanol ($C_2H_5O^+$), 1-propanol ($C_3H_8O^+$) and 1-butanol ($C_4H_{10}O^+$) that resulted from electron impact ionization. On the right side of this figure, is shown the amplified parent ion PICS of 1-butanol. This is done so that the reader can observe the similar shape behaviour of its PICS to the other alcohols. The intensity ratio of these curves shows the dramatic drop in the parent ion cross sections, as the carbon chain increases, indicating the possibility of new alcohol breakdown routes. This latter fact becomes apparent if one also observes comparatively their mass spectra (Fig. 1), where we find clear growth in the production of other cations as the linear carbon chain increases. In Figure 4, on the left pane, we show the PICS for the mass 31 amu of oxonium, for electron impact in the energy range 10–100 eV on the C_1–C_4 alcohols. In this figure we observed that the cross section for oxonium formation for 1-propanol (5.52×10^{-16} cm^2) is remarkably bigger compared to the other alcohols, which are 2.65×10^{-16} cm^2 for ethanol, 2.24×10^{-16} cm^2 for 1-butanol, and 1.643×10^{-16} cm^2 for methanol. There is a systematic growth in the production of this ion as the carbon chain grows from methanol to propanol (C_1–C_3). On the other hand for 1-butanol (C_4), there occurs a change in the fragmentation pattern, observing a transference in the fragmentation probability (cross section) to other fragments such as $C_3H_5^+$ (41 amu), shown on the right hand side of Figure 4. Note that the Appearance Energy for the C_4 oxonium cation was registered at 11.76 ± 0.02 eV, while that for the cation $C_3H_5^+$ (41 amu) was at 11.42 ± 0.18 eV, as will be discussed next, suggesting that the formation of these two cations could come from the same reaction channel. This behaviour indicates that the fragmentation is more spontaneous in the larger alcohols, which may be a much-desired feature for a biofuel, when more complete combustion is expected to occur, which would allow poorer fuel-air mixtures in vehicle engines. This could ultimately result in more economical vehicles.

From measurements of near-threshold PICS curves, the ionization energy (IE) of the parent ion and the AEs of the other cation fragments were obtained by fitting the extended Wannier Law [64,65], convoluted with the experimental instrument response function [2] i.e. the energy spread of incident electron. The derived AEs, for those most prominent cations observed in the mass spectra of C_1–C_4 alcohols reported by us in [1–4], are listed in Table 4. The parent ion of methanol, ethanol, 1-propanol and 1-butanol were found to have AEs of 10.7 ± 0.1 eV,

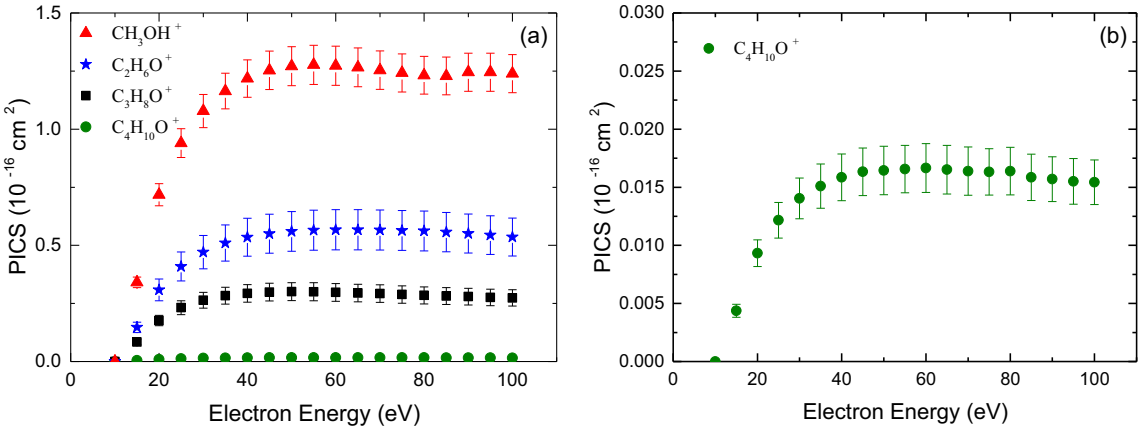

Fig. 3. (a) Absolute partial ionization cross sections (PICS) of the parent C_1–C_4 alcohols and (b) amplified PICS for C_4 that resulted from electron impact ionization reported by [1–4]. The errors are the quadrature sum of (i) the uncertainty in the experimental measurements of the cross sections, (ii) the uncertainty of the relative contributions to the mass spectrum and (iii) the normalization to the absolute data of Rejoub et al. [20] for ethanol, methanol and 1-propanol, and of Hudson et al. [36] for 1-butanol. See also legend in figure.

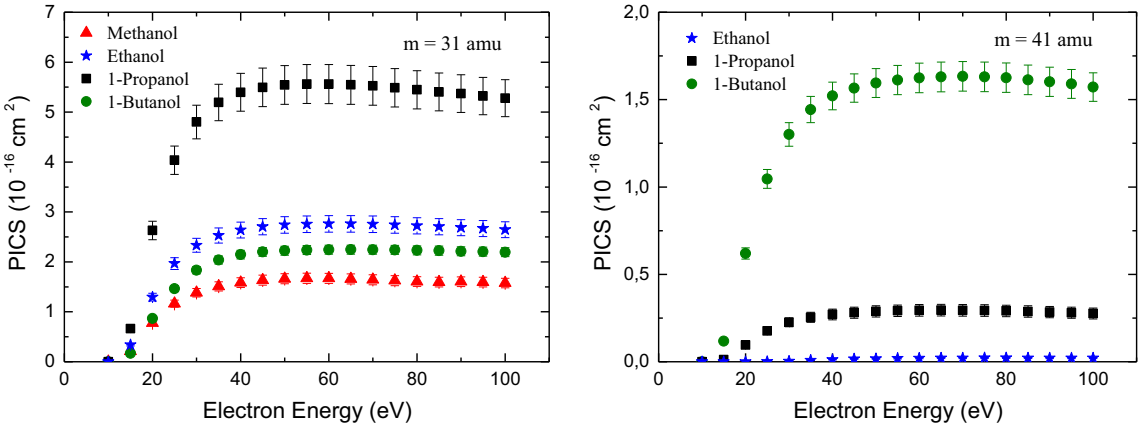

Fig. 4. PICS of the 31 amu (oxonium) and 41 amu mass cation production for C_1–C_4 primary alcohols reported by [1–3]. See also legend in figure.

10.4 ± 0.1 eV, 10.48 ± 0.01 eV and 10.27 ± 0.03 eV, in good agreement with the values reported by NIST [61]. The other AEs determined by [1–3] are typically in excellent agreement with the values available from NIST, with some few exceptions such as the AE for $C_2H_3^+$ (m = 27 amu) in 1-propanol [2], registered at 13.42 ± 0.18, which is 7.5% lower than the value reported by NIST [61].

Finally, we observed that the determination of AE values from recorded PICS curves may be very useful for assigning the formed cations in the electron collision with a molecule, i.e. the peaks recorded in the mass spectrum [1–4]. For masses where multiple-distinct cation formation is possible, when fitting two AE values should be found, validating their formation. This is the case observed for the 28 amu 1-butanol mass, where two AE values were found (10.94 ± 0.03 eV and 12.34 ± 0.11 eV), that are associated with the formation of CO^+ and $C_2H_4^+$ cations. In the case where the fitting process registers two distinct AE values for a single cation (mass), it is clear that this reflects the formation of distinct isomers or the formation of a single cation through different mechanisms. For example, in the determination of the AEs for masses 44 amu and 45 amu for 1-propanol, in the fitting procedure there are two different fragmentation channels available [3]. For mass 44 amu was found the AEs at 10.53 eV and 13.27 eV due to production of two different molecules, $C_3H_8^+$ or $C_2H_4O^+$, while for mass 45 amu, was found AEs at 11.33 eV and 13.03 eV due the formation of two $C_2H_5O^+$ isomers (CH_3-$CH{=}O^+H$ or $CH_2{=}O^+$-CH_3) [3].

4 Conclusions

A review of recent investigations of the primary alcohols methanol, ethanol, 1-propanol and 1-butanol was presented in this work, encompassing the measurement of the cation mass spectrum for a fixed electron impact energy (70 eV), and the absolute partial ionization cross sections for the electron impact energy range from 10 to 100 eV. Well-resolved mass peaks in the mass spectra have

Table 4. Comparison of the appearance energies (in eV) of the most abundant cations formed in electron collisions with methanol [1], ethanol [1], 1-propanol [2] and 1-butanol [3].

	Methanol		Ethanol		Propanol		Butanol	
Mass	Cation	AE	Cation	AE	Cation	AE	Cation	AE
12					C^+	22.32 ± 0.34	C^+	22.27 ± 0.15
14	CH_2^+	14.1 ± 0.1					CH_2^+	15.27 ± 0.12
15	CH_3^+	14.0 ± 0.1	CH_3^+	14.0 ± 0.1			CH_3^+	10.16 ± 0.13
								14.56 ± 0.10
26			$C_2H_2^+$	11.3 ± 0.1	$C_2H_2^+$	10.99 ± 0.27	$C_2H_2^+$	11.60 ± 0.07
27					$C_2H_3^+$	13.42 ± 0.18	$C_2H_3^+$	13.63 ± 0.05
28			CO^+ or $C_2H_4^+$	10.5 ± 0.1	CO^+ or $C_2H_4^+$	11.33 ± 0.11	CO^+ or $C_2H_4^+$	10.94 ± 0.03
								12.34 ± 0.11
29			COH^+or $C_2H_5^+$	12.1 ± 0.1	COH^+ or $C_2H_5^+$	12.26 ± 0.06	COH^+ or $C_2H_5^+$	8.91 ± 0.13
								12.57 ± 0.10
30	CH_2O^+	10.6 ± 0.1	CH_2O^+ or $C_2H_6^+$	10.3 ± 0.1	CH_2O^+ or $C_2H_6^+$	10.66 ± 0.23	CH_2O^+ or $C_2H_6^+$	11.08 ± 0.11
31	CH_2OH^+	11.1 ± 0.1	CH_2OH^+	10.7 ± 0.1	CH_2OH^+	11.60 ± 0.02	CH_2OH^+	11.76 ± 0.02
32	CH_4O^+	10.7 ± 0.1	CH_4O^+	10.8 ± 0.1			CH_4O^+	11.09 ± 0.03
33							CH_5O^+	11.60 ± 0.01
37							C_3H^+	16.26 ± 0.55
38							$C_3H_2^+$	13.25 ± 0.30
39					$C_3H_3^+$	11.44 ± 0.16	$C_3H_3^+$	10.71 ± 0.09
40					C_2O^+ or $C_3H_4^+$	10.45 ± 0.05	C_2O^+ or $C_3H_4^+$	11.52 ± 0.04
41					C_2HO^+ or $C_3H_5^+$	8.08 ± 0.79	C_2HO^+ or $C_3H_5^+$	8.09 ± 0.46
						12.54 ± 0.05		11.42 ± 0.18
42			$C_2H_2O^+$	9.6 ± 0.1	$C_2H_2O^+$ or $C_3H_6^+$	10.62 ± 0.01	$C_2H_2O^+$ or $C_3H_6^+$	11.49 ± 0.03
43			$C_2H_3O^+$	9.8 ± 0.1	$C_2H_3O^+$ or $C_3H_7^+$	10.59 ± 0.05	$C_2H_3O^+$ or $C_3H_7^+$	11.65 ± 0.03
44			$C_2H_4O^+$	10.1 ± 0.1	$C_2H_4O^+$ or $C_3H_8^+$	10.53 ± 0.65	$C_2H_4O^+$ or $C_3H_8^+$	10.67 ± 0.02
						13.27 ± 0.56		12.11 ± 0.07
45			$C_2H_5O^+$	10.5 ± 0.1	$C_2H_5O^+$	11.33 ± 0.42	$C_2H_5O^+$	11.72 ± 0.01
						13.03 ± 0.17		13.16 ± 0.20
46			$C_2H_6O^+$	10.4 ± 0.1			$C_2H_6O^+$	11.30 ± 0.08
47							$C_2H_7O^+$	12.21 ± 0.12
50							$C_4H_2^+$	10.60 ± 0.13
								13.12 ± 0.65
51							$C_4H_3^+$	12.80 ± 0.18
52							$C_4H_4^+$ or C_3O^+	9.97 ± 0.09
53							$C_4H_5^+$ or C_3HO^+	9.91 ± 0.05
								12.28 ± 0.28
54							$C_4H_6^+$ or $C_3H_2O^+$	9.63 ± 0.09
55							$C_4H_7^+$ or $C_3H_3O^+$	11.61 ± 0.02
56							$C_4H_8^+$ or $C_3H_4O^+$	10.48 ± 0.01
57							$C_4H_9^+$ or $C_3H_5O^+$	10.56 ± 0.03
58							$C_3H_6O^+$	10.72 ± 0.15
59					$C_3H_7O^+$	10.76 ± 0.02	$C_3H_7O^+$	11.24 ± 0.11
60					$C_3H_8O^+$	10.48 ± 0.01	$C_3H_8O^+$	10.93 ± 0.16
72							$C_4H_8O^+$	10.12 ± 0.04
73							$C_4H_9O^+$	11.14 ± 0.07
74							$C_4H_{10}O^+$	10.27 ± 0.03

been obtained by several authors, and their relative abundances and cation assignments have also been reported by [1–3]. The mass spectra for the C_1–C_4 alcohols reported by [1–3] were found to be in pretty good agreement with the earlier data reported by NIST [61]. The methanol spectrum [1] also compared quite well with data from Srivastava et al. [34]. However, for this species some differences are observed with the data obtained by Douglas and Price [42] and Cummings and Bleakney [43]. Good agreement was also found for the relative ratio intensities in the 1-propanol spectrum reported by Pires et al. [2] and Maccoll [47]. The 1-butanol spectrum reported by Pires et al. [2] showed a large number of low intensity cations peaks observed for the first time. Total ionization cross section data were also calculated using the BEB, IAM-SCAR and semi-classical Deutsch-Märk (DM) methods by [2,4]. These results were compared to experimental data [2,4] observing a good overall agreement to the BEB calculations. Agreement with the IAM-SCAR and DM computations was less satisfactory, although the IAM-SCAR did qualitatively reproduce the experimental results over the common energy range. Finally we note a recent plane wave Born approximation calculation, using continuum generalised oscillator strengths [18], from Kumar et al. [66], for the TICS of methanol, ethanol and 1-propanol. Those results are typically in very good accord, with the measured UFJF cross sections [1–3], to within the uncertainty on the data.

Additionally, the appearance energies of the identified cations were also determined by [1–3] and found to be in generally fair agreement with the NIST sourced data. The comparison between the absolute partial ionization cross sections of the primary alcohols from C_1 to C_4, from [1–3] and that of previous work, indicates some differences in the cross sections for like cations, thus providing more knowledge about the fragmentation process in each case. Among the primary alcohols of C_1 to C_4 the 1-butanol molecule has been identified as one of the most promising to be used to replace fossil fuels. This follows as it can release more chemical energy, in the form of heat, during ignition and it will not need modifications to engine components if used instead of gasoline [3,4]. Therefore, the investigations reported here on the primary alcohols contributed new experimental data that will be required if we are to further understand and optimize the ignition process, required for the efficient and cost-competitive

utilization of the primary alcohols as alternate fuels.

This work was supported by the Brazilian Conselho Nacional de Desenvolvimento Cientifico e Tecnológico (CNPq), Fundação de Amparo à Pesquisa do Estado de Minas Gerais (FAPEMIG) and FINEP. M.C.A.L. acknowledges financial support from CNPq, while W.A.D.P., S. G., A.C.P.F. and R.A.A.A. acknowledge their fellowships from CAPES. Some financial assistance from the Australian Research Council through grant # DP180101655 is also noted. Finally, G. Garcia thanks the Spanish Ministerio de Economia, Industria y Competitividad for his project grant FIS 2016-80440 and the EU project FP7 – ITN – ARGENT - 608163.

Author contribution statement

All authors contributed equally to the paper.

Publisher's Note The EPJ Publishers remain neutral with regard to jurisdictional claims in published maps and institutional affiliations.

References

1. K.L. Nixon, W.A.D. Pires, R.F.C. Neves, H.V. Duque, D.B. Jones, M.J. Brunger, M.C.A. Lopes, Int. J. Mass Spectrom. **404**, 48 (2016)
2. W.A.D. Pires, K.L. Nixon, S. Ghosh, R.F.C. Neves, H.V. Duque, R.A.A. Amorim, D.B. Jones, F. Blanco, G. Garcia, M.J. Brunger, M.C.A. Lopes, Int. J. Mass Spectrom. **422**, 32 (2017)
3. W.A.D. Pires, K.L. Nixon, S. Ghosh, R.A.A. Amorim, R.F.C. Neves, H.V. Duque, D.G.M. da Silva, D.B. Jones, M.J. Brunger, M.C.A. Lopes, Int. J. Mass Spectrom. **430**, 158 (2018)
4. S. Ghosh, K.L. Nixon, W.A.D. Pires, R.A.A. Amorim, R.F.C. Neves, H.V. Duque, D.G.M. da Silva, D.B. Jones, F. Blanco, G. Garcia, M.J. Brunger, M.C.A. Lopes, Int. J. Mass Spectrom. **430**, 44 (2018)
5. S. Payne, T. Dutzik, E. Figdor, Environment America Research and Policy Center http://www.environmentamerica.org/sites/environment/files/reports/The-High-Cost-of-Fossil-Fuels (2009)
6. B. Pieprzyk, N. Kortlüke, P.R. Hilje, Energy Research Architecture Report – European Biodiesel Board, 225, 2009
7. World Health Organization, *How Air Pollution is Destroying our Health* https://wwwwhoint/air-pollution/news-and-events/how-air-pollution-is-destroying-our-health (2019)
8. P. Sabuco, *BNP Paribas Specialized Trade Solutions, The future of alternative fuel-powered cars*, https://focusmagazine.bnpparibas (2019)
9. M.A. Ridenti, J.A. Filho, M.J. Brunger, R.F. da Costa, M.T. do, N. Varella, M.H.F. Bettega, M.A.P. Lima, Eur. Phys. J. D **70**, 161 (2016)
10. M.J. Brunger, Int. Rev. Phys. Chem. **36**, 333 (2017)
11. *Biofuels the Fuel of the Future*, http://biofuel.org.uk/ for information on types of biofuels, advantages and disadvantages when compared to fossil fuels
12. B. Ndaba, I. Chiyanzu, S. Marx, Biotechnol. Rep. **8**, 1 (2015)
13. *Technology Collaboration Programme on Advanced Motor Fuels*, http://www.iea-amf.org/content/fuel_information/butanol/properties#octane_numbers, for information on advanced motor fuels
14. W. Han, C. Yao, Fuel **150**, 29 (2015)
15. P. Oßwald, H. Güldenberg, K. Kohse-Höinghaus, B. Yang, T. Yuan, F. Qi, Combust. Flame **158**, 2 (2011)
16. M.A. Khakoo, J. Muse, H. Silva, M.C.A. Lopes, C. Winstead, V. McKoy, E.M. de Oliveira, R.F. da Costa, M.T. do N. Varella, M.H.F. Bettega, M.A.P. Lima, Phys. Rev. A **78**, 062714 (2008)
17. A.P. Mariano, N. Qureshi, R. Maciel Filho, T.C. Ezeji, Biotechnol. Bioeng. **108**, 1757 (2011)
18. H. Tanaka, M.J. Brunger, L. Campbell, H. Kato, M. Hoshino, A.R.P. Rau, Rev. Mod. Phys. **88**, 025004 (2016)
19. F. Schmieder, Z. Elektrochem. Angew. Phys. Chem. **36**, 700 (1930)
20. R. Rejoub, C.D. Morton, B.G. Lindsay, R.F. Stebbings, J. Chem. Phys. **118**, 1756 (2003)
21. O. Sueoka, Y. Katayama, S. Mori, At. Coll. Res. Japan Prog. Rep. **11**, 17 (1985)
22. C. Szmytkowski, A.M. Krzysztofowicz, J. Phys. B: At. Mol. Opt. Phys. **28**, 4291 (1995)
23. M. Vinodkumar, C. Limbachiya, K.N. Joshipura, B. Vaishnav, S. Gangopadhyay, J. Phys. Conf. Ser. **115**, 012013 (2008)
24. D.G.M. Silva, T. Tejo, J. Muse, D. Romero, M.A. Khakoo, M.C.A. Lopes, J. Phys. B: At. Mol. Opt. Phys. **43**, 015201 (2010)
25. X.M. Tan, D.H. Wang, Nucl. Instrum. Methods Phys. Res. B **269**, 1094 (2011)
26. M.T. Lee, G.L.C. de Souza, L.E. Machado, L.M. Brescansin, A.S. dos Santos, R.R. Lucchese, R.T. Sugohara, M.G.P. Homem, I.P. Sanches, I. Iga, J. Chem. Phys. **136**, 114311 (2012)
27. M. Vinodkumar, C. Limbachiya, A. Barot, N. Mason, Phys. Rev. A **87**, 012702 (2013)
28. D.G.M. da Silva, M. Gomes, S. Ghosh, I.F.L. Silva, W.A.D. Pires, D.B. Jones, F. Blanco, G. Garcia, S.J. Buckman, M.J. Brunger, M.C.A. Lopes, J. Chem. Phys. **147**, 194307 (2017)
29. M. Gomes, D.G.M. da Silva, A.C.P. Fernandes, S. Ghosh, W.A.D. Pires, D.B. Jones, G. García, M.J. Brunger, M.C.A. Lopes, J. Chem. Phys. **150**, 194307 (2019)
30. D. Bouchiha, J.D. Gorfinkiel, L.G. Caron, L. Sanche, J. Phys. B: At. Mol. Opt. Phys. **40**, 1259 (2007)
31. M.A. Khakoo, J. Blumer, K. Keane, C. Campbell, H. Silva, M.C.A. Lopes, C. Winstead, V. McKoy, R.F. da Costa, L.G. Ferrira, M.A.P. Lima, M.H.F. Bettega, Phys. Rev. A **77**, 042705 (2008)
32. R.T. Sugohara, M.G.P. Homem, I.P. Sanches, A.F. de Moura, M.T. Lee, I. Iga, Phys. Rev. A **83**, 032708 (2011)
33. N. Duric, I. Cadez, M.V. Kurepa, Fizika **21**, 339 (1989)
34. S.K. Srivastava, E. Krishnakumar, A.F. Fucaloro, T. van Note, J. Geophys. Res. **101**, 26155 (1996)
35. H. Deutsch, K. Becker, R. Basner, M. Schmidt, T.D. Märk, J. Phys. Chem. A **102**, 8819 (1998)
36. J.E. Hudson, M.L. Hamilton, C. Vallance, P.W. Harland, Phys. Chem. Chem. Phys. **5**, 3162 (2003)
37. S. Pal, Chem. Phys. **302**, 119 (2004)

38. M. Vinodkumar, K. Korot, P.C. Vinodkumar, Int. J. Mass. Spectrom. **305**, 26 (2011)
39. J.N. Bull, P.W. Harland, C. Vallance, J. Phys. Chem. A **116**, 767 (2012)
40. N. Uddin, P. Verma, M.J. Alam, S. Ahmad, B. Antony, Int. J. Mass. Spectrom. **432**, 37 (2018)
41. A.N. Zavilopulo, F.F. Chipev, L.M. Kokhtych, Nucl. Instrum. Methods Phys. Res. B **233**, 302 (2005)
42. K.M. Douglas, S.D. Price, J. Chem. Phys. **131**, 224305 (2009)
43. C.S. Cummings, W. Bleakney, Phys. Rev. **58**, 787 (1940)
44. J.M. Williams, W.H. Hamill, J. Chem. Phys. **49**, 4467 (1968)
45. E. Szot, L. Wójcik, K. G1uch, Vacuum **90**, 141 (2013)
46. E. Szot, K. Gauch, L. Wójcik, Acta Phys. Pol. A **123**, 797 (2013)
47. A. Maccoll, Org. Mass Spectrom **21**, 601 (1986)
48. R.A. Friedel, L. Shultz, A.G. Sharkey Jr., Anal. Chem. **8**, 45 (1956)
49. S. Beck, A. Michalski, O. Raether, M. Lubeck, S. Kaspar, N. Goedecke, C. Baessmann, D. Hornburg, F. Meier, I. Paron, N.A. Kulak, J. Cox, M. Mann, Molecular & Cellular Proteomics **14**, 2014 (2015)
50. *Hidden Analytical*, http://www.hidenanalytical.com.en/ for a description of the mass spectrometer
51. F. Blanco, G. Garcia, J. Phys. B: At. Mol. Opt. Phys. **42**, 145203 (2009)
52. O. Zatsarinny, K. Bartschat, G. Garcia, F. Blanco, L.R. Hargreaves, D.B. Jones, R. Murrie, J.R. Brunton, M.J. Brunger, M. Hoshino, S.J. Buckman, Phys. Rev. A **83**, 042702 (2011)
53. D. Wandschneider, M. Michalik, A. Heintz, J. Mol. Liq. **125**, 2 (2006)
54. M.J. Frisch et al., *Gaussian 09, Revision B.* (2010), Vol. 1
55. R.D. Cowan, *The Theory of Atomic Structure and Spectra* (University of California Press, London, 1981)
56. M.E. Riley, D.G. Truhlar, J. Chem. Phys. **63**, 2182 (1975)
57. X. Zhang, J. Sun, Y. Liu, J. Phys. B: At. Mol. Opt. Phys. **25**, 1893 (1992)
58. F. Blanco, G. García, Phys. Lett. A **295**, 178 (2002)
59. J. Greaves, J. Roboz, *Mass Spectrometry for the Novice* (CRC Press, London, 2013)
60. E. Szot, L. Wójcik, K. G1uch, Vacuum **90**, 141 (2013)
61. *NIST Webbook, NIST Chemistry WebBook, NIST Standard Reference Database, Number 69*, edited by P.J. Linstrom, W.G. Mallard, http://webbook.nist.gov, which provides the mass spectra for C1-C4 alcohols
62. A. Maccoll, Org. Mass Spectrom. **21**, 601 (1986)
63. R.A. Friedel, J.L. Shultz, A.G. Sharkey, Anal. Chem. **28**, 926 (1956)
64. T. Fiegele, G. Hanel, I. Torres, M. Lezius, T.D. Märk, J. Phys. B: At. Mol. Opt. Phys. **33**, 4263 (2000)
65. S. Denifl, B. Sonnweber, G. Hanel, P. Scheier, T.D. Märk, Int. J. Mass. Spectrom. **238**, 47 (2004)
66. Y. Kumar, M. Kumar, S. Kumar, R. Kumar, Atoms **1**, 60 (2019)